INTERNATIONAL JOURNAL FOR NUMERICAL METHODS IN ENGINEERING, VOL. 17, 1497–1514 (1981)

A GENERAL FORMULATION FOR COUPLED THERMAL FLOW OF METALS USING FINITE ELEMENTS

O. C. ZIENKIEWICZ†
University of Wales, University College of Swansea, U.K.

E. OÑATE‡
Ing. de Caminos, Polytechnic of Barcelona, Barcelona, Spain

J. C. HEINRICH§
University of Arizona, Tucson, Arizona, U.S.A.

SUMMARY

A finite element formulation to deal with the flow of metals coupled with thermal effects is presented. The deformation process of the metal is treated using the visco-plastic flow approach and the solution technique for the coupled problem implies a simultaneous solution for velocities and temperatures. Some aspects of the numerical solution of the problem are given and in the last part of the paper some examples of steady-state extrusion and rolling problems showing the applicability of the method are shown.

INTRODUCTION

In most metal forming processes the total strains are so large that the elastic deformation can be considered as negligible versus the plastic or viscoplastic strains, and the state of deformation can be considered as given by a constitutive law which defines the strain rate as a non-zero function of stresses

$$\dot{\varepsilon}_{ij} = f(\sigma_{kl}) \tag{1}$$

In such cases, the deformation process is equivalent to the flow of a viscous fluid of a non-Newtonian kind.

This procedure, commonly known as the 'flow approach', was first presented in the work of Goon *et al.*[1] Zienkiewicz and Godbole[2,4] gave a more general solution for viscoplastic materials. Many authors[5,9] have presented solutions for pure plasticity which prove that the flow formulation is a valuable technique for modelling of metal forming processes.

In general, it is clear that the assumption that metal forming processes are isothermal is not tenable, and unlikely to be a good approximation as the deformations are very large and temperature changes occur either due to external/internal sources of heat, or due to the spontaneous heat generation following the energy dissipation in the plastic deformation process. In such cases, if the material is temperature sensitive, the deformation process is highly coupled with the energy balance equation.

† Professor of Civil Engineering.
‡ Lecturer, E.T.S.
§ Associate Professor.

0029–5981/81/101497–18$01.80

Received 3 November 1980
Revised 11 December 1980

The extension of the general 'flow approach' to take into account prescribed temperature conditions is trivial. Clearly, if the temperature is known *a priori* and its relation to the yield stress is given, no additional difficulties are introduced in the nonlinear flow solution. This, indeed, has been done by Cornfield and Johnson[5] in the development of a numerical solution for hot rolling problems, and extended to the process of dieless extrusion by Price and Alexander.[9] Of more complexity is the problem of determining the coupling due to the energy dissipation, which in turn is dependent on temperature sensitive yield values. Nearly all the energy dissipated in the plastic deformation process is converted into heat energy and causes the temperature of the material to rise. Farren and Taylor[10] measured both the plastic work and the temperature rise in a tensile experiment. They found that for steels, copper and aluminium, the heat rise represents 86·5, 90·5–92 and 95 per cent, respectively, of the plastic work. The remainder of the plastic work is stored as internal energy associated with the small scale non-homogeneous deformations that are inherent characteristics of plastic flow. This energy can be recovered during heat treatment. It is obvious, therefore, that the temperature rise in a plastic deformation process must be considerable, and that the problem of the temperature development must be studied in conjunction with the flow process.

The first attempt to solve numerically the thermal problem of plastic deformation was made by Bishop[12] who developed a numerical method to compute the temperature distribution associated with a plane extrusion problem. He assumed the material to be perfectly rigid plastic and obtained the flow field from a slip line solution. Such a solution required the yield stress to be independent of rate and temperature, hence his numerical solution is an uncoupled thermoplastic one. Later, Altan and Kobayashi[13] applied Bishop's method for finding the temperature field for the case of axisymmetric extrusion. They obtained the deformation field through experimental 'visioplasticity' methods[14] and they used a constitutive equation sensitive to both temperature and strain rates. Therefore, their solution is essentially uncoupled. Basically, the above methods worked in Eulerian co-ordinates and made the approximation that the process was resolved into two steps, one involving heat generation and transport (convection) and the other conduction. More recently Sulijoadikusomo and Dillon[15] have calculated the temperature distribution during a transient axisymmetric extrusion process for a material with temperature-sensitive properties. To calculate the deformation gradient field again experimental methods were used; therefore, the flow solution was not attempted analytically and the procedure is similar to that of Altan and Kobayashi but with a Lagrangian approach instead of an Eulerian one.

The first attempt to use the flow formulation for solving coupled thermal plastic problems was made by Zienkiewicz *et al.*[16] and Jain[17] who used a finite element iterative procedure which follows the lines of (a) solving the flow problem for a given temperature distribution, (b) solution of the thermal equations for which temperatures are calculated, and (c) repetition of the solution of the flow problem with the plasticity values adjusted according to the temperature field. They applied this method to find the temperature distribution for a plane extrusion problem.

In this paper a direct coupled thermal plastic/viscoplastic flow numerical solution algorithm using finite elements is presented. The solution for the temperature distribution is obtained simultaneously with that for the velocity field. In particular, the general formulation is presented in more detail for steady-state coupled thermal creeping plastic/viscoplastic flow problems. The discrete systems of equations for the velocity and temperature fields are obtained by applying the Galerkin weighted residuals method to the equilibrium equations and to the heat balance equations, respectively.[11,18] The incompressibility constraint is imposed via a penalty function method. The flow and temperature equations are simultaneously solved using a non-symmetric solver.

The element used throughout this paper is the nine-noded isoparametric Lagrangian quadrilateral with biquadratic shape functions for velocities and temperature. A selective integration scheme is employed in the evaluation of the terms of the stiffness matrix due to flow. Some aspects of the numerical solution are discussed, and in the last part of the paper some examples of steady-state plane and axisymmetric extrusion and hot rolling problems are presented.

CONSTITUTIVE RELATIONS FOR A VON MISES TYPE FLOW

If elastic deformations are neglected a general description of behaviour of most materials can be given in terms of viscoplasticity with the strain rates defined by a relationship of the form

$$\dot{\varepsilon}_{ij} = \Gamma_{ijkl}\sigma_{kl} \tag{2}$$

where

$$\Gamma_{ijkl} = \Gamma(\varepsilon_{kl}, T) \tag{3}$$

is a symmetric tensor and T is the temperature.

For a Von Mises type of plastic or viscoplastic material, applicable to metals and many other materials, the form of matrix Γ can be easily obtained using Perzyna's viscoplasticity model, and equation (2) as shown by Zienkiewicz and Cormeau[19] can be written in a manner describing an isotropic incompressible non-Newtonian fluid with[7,16]

$$\dot{\varepsilon}_{ij} = \frac{1}{2\mu} s_{ij}; \qquad s_{ij} = \sigma_{ij} - \delta_{ij}p \qquad p = \sigma_{ii}/3 \tag{4}$$

with

$$\mu = \frac{\sigma_y + (\dot{\bar{\varepsilon}}/\gamma\sqrt{3})^{1/n}}{\sqrt{3}\dot{\bar{\varepsilon}}} \tag{5}$$

In the above, μ is the nonlinear viscosity, p is the pressure, γ and s are physical constants for viscoplastic materials,[19] σ_y is the uniaxial yield stress of the material, which in general is a function of the temperature, pressure, and deviatoric strain invariant $\bar{\varepsilon}$. The rate of $\bar{\varepsilon}$ is defined here as

$$\dot{\bar{\varepsilon}} = \sqrt{(2\dot{\varepsilon}_{ij}\dot{\varepsilon}_{ij})} \tag{6}$$

For pure plastic flow the value of γ tends to infinity; therefore equation (5) yields

$$\mu = \frac{\sigma_y}{\sqrt{(3)}\dot{\bar{\varepsilon}}} \tag{7}$$

It is important to notice that for small values of $\dot{\bar{\varepsilon}}$ the viscosity tends to infinity; therefore in numerical computation a cut-off value must be chosen.†

† If the strain invariant, $\bar{\varepsilon}$, is defined as is common in literature by

$$\dot{\bar{\varepsilon}} = \sqrt{(\tfrac{2}{3}\dot{\varepsilon}_{ij}\dot{\varepsilon}_{ij})}$$

equations (5) and (7) must be subsequently modified to give

$$\mu = \frac{\sigma_y + (\dot{\bar{\varepsilon}}/\gamma)^{1/n}}{3\dot{\bar{\varepsilon}}}$$

and

$$\mu = \frac{\sigma_y}{3\dot{\bar{\varepsilon}}}$$

COUPLED THERMAL PLASTIC/VISCOPLASTIC FLOW: BASIC EQUATIONS

As we have already said, in metal forming the deformation process is highly coupled with the energy balance equations. In this, the temperature development depends on the energy dissipation occurring in the plastic process at a rate given by

$$Q = \frac{f}{J}\sigma_{ij}\dot{\varepsilon}_{ij} \tag{8}$$

where f is the fraction of plastic work that turns into heat and J is the mechanical equivalent of heat.

This energy enters the thermal diffusion–convection equation

$$\rho c\left[\frac{\partial T}{\partial t} + (\nabla T)^{\mathrm{T}}\mathbf{u}\right] = \nabla^{\mathrm{T}}(k\nabla T) + Q \tag{9}$$

where T is the temperature, $\partial/\partial t$ the time derivative, ρ the density, k the conductivity, and c the specific heat per unit volume.

Equation (9) must be solved simultaneously with the incompressible flow equations. These are

(1) Equilibrium $$\mathbf{L}^{\mathrm{T}}\boldsymbol{\sigma} + \mathbf{b}_0 - \rho\left[\frac{\partial \mathbf{u}}{\partial t} + (\nabla \mathbf{u})^{\mathrm{T}}\mathbf{u}\right] = 0 \tag{10}$$

(2) Incompressibility $$\mathbf{m}^{\mathrm{T}}\dot{\boldsymbol{\varepsilon}} = 0 \tag{11}$$

In the above, $\mathbf{b}$ are constant body forces, $\boldsymbol{\sigma}$ and $\dot{\boldsymbol{\varepsilon}}$ are the stress and strain rate tensors, respectively, written in vector form, $\mathbf{u}$ is the true velocity vector, $\nabla = [\partial/\partial x, \partial/\partial y]^{\mathrm{T}}$ for plane and axisymmetric situations, and $\mathbf{L}$ and $\mathbf{m}$ are matrix operators which can be found in Reference 20.

The stresses, $\boldsymbol{\sigma}$ are related to the strain rate using equation (4) and retaining the mean pressure as

$$\boldsymbol{\sigma} = -\mathbf{m}p + \mu\mathbf{D}\dot{\boldsymbol{\varepsilon}} \tag{12}$$

Here the strain rate $\dot{\boldsymbol{\varepsilon}}$ is defined as

$$\dot{\boldsymbol{\varepsilon}} = \mathbf{L}\mathbf{u} \tag{13}$$

The particular forms of $\mathbf{D}$ for plane and axisymmetric problems can be found in texts.[20] The system is completed by equation (5) and suitable expressions for the temperature dependence of the physical properties.

The boundary conditions which need to be specified here are either the velocities

$$\mathbf{u} = \bar{\mathbf{u}} \tag{14a}$$

or tractions

$$\mathbf{t} = \bar{\mathbf{t}} \tag{14b}$$

and the temperature

$$T = \bar{T} \tag{14c}$$

or heat flow

$$-k\mathbf{n}^{\mathrm{T}}\nabla T = q + \alpha(T - \bar{T}) \tag{14d}$$

In the above, the bar denotes a specified boundary value, $\mathbf{n}$ is the outward normal to the boundary and α is a radiation coefficient.

Discretization of the thermal flow equations

The finite element discretization of equations (9); (10) and (11) follows standard patterns.[20] The velocity and temperature fields are expressed in terms of independent nodal parameters and suitable shape functions as

$$\begin{aligned} \mathbf{u} &= \Sigma \mathbf{N}_i \mathbf{a}_i = \mathbf{N}\mathbf{a} \\ T &= \Sigma \bar{N}_i T_i = \bar{\mathbf{N}}\mathbf{T} \end{aligned} \tag{15}$$

where for plane and axisymmetric flow (see Appendix I)

$$\mathbf{u} = [u, v]^{\mathrm{T}}; \qquad \mathbf{a}_i = [u_i, v_i] \tag{16}$$

Applying the Galerkin method with weighting functions $\mathbf{W}$ and $\bar{\mathbf{W}}$, respectively, to equations (10) and (9) and rewriting equation (11) in discrete form we have

$$\int_\Omega \hat{\mathbf{B}}^{\mathrm{T}} \boldsymbol{\sigma}\, \mathrm{d}\Omega + \left[\int_\Omega \rho \mathbf{W}^{\mathrm{T}} (\nabla (\mathbf{N}\mathbf{a})^{\mathrm{T}})^{\mathrm{T}} \mathbf{N}\, \mathrm{d}\Omega\right] \mathbf{a} \tag{17}$$

$$+ \left[\int_\Omega \mathbf{W}^{\mathrm{T}} \rho \mathbf{N}\, \mathrm{d}\Omega\right] \frac{\mathrm{d}}{\mathrm{d}t}\mathbf{a} - \int_\Omega \mathbf{W}^{\mathrm{T}} \mathbf{b}_0\, \mathrm{d}\Omega - \int_{\Gamma_t} \mathbf{W}^{\mathrm{T}} \bar{t}\, \mathrm{d}\Gamma = 0 \tag{18}$$

$$\left[\int_\Omega \{\rho c \bar{\mathbf{W}}^{\mathrm{T}} (\nabla \bar{\mathbf{N}}^{\mathrm{T}})^{\mathrm{T}} \mathbf{N}\mathbf{a} + k \nabla \bar{\mathbf{W}}^{\mathrm{T}} \nabla \bar{\mathbf{N}}\}\, \mathrm{d}\Omega + \int_{\Gamma_q} \alpha \bar{\mathbf{W}}^{\mathrm{T}} \bar{\mathbf{N}}\, \mathrm{d}\Gamma\right] \mathbf{T}$$

$$+ \left[\int_\Omega \rho c \bar{\mathbf{W}}^{\mathrm{T}} \bar{\mathbf{N}}\right] \frac{\mathrm{d}\mathbf{T}}{\mathrm{d}t} - \int_\Omega \bar{\mathbf{W}}^{\mathrm{T}} Q\, \mathrm{d}\Omega + \int_{\Gamma_q} \bar{\mathbf{W}}^{\mathrm{T}} (\bar{q} - \alpha \bar{T})\, \mathrm{d}\Gamma = 0 \tag{19}$$

In the above, $\hat{\mathbf{B}} = \mathbf{L}\mathbf{W}$, $\mathbf{B} = \mathbf{L}\mathbf{N}$ and $\bar{t}, q$ are prescribed tractions and heat flows on the surfaces Γ_t and Γ_q, respectively.

In this paper the incompressibility constraint, equation (18), has been treated using a 'penalty function' approach[18] which allows us to eliminate the pressure, p, writing equation (18) as

$$\mathbf{m}^{\mathrm{T}} \mathbf{B}\mathbf{a} = p/\lambda \tag{20}$$

where λ is a very large quantity (generally this is taken as $10^7\ \mu$). The above equation gives automatically

$$p = \lambda\, \mathbf{m}^{\mathrm{T}} \mathbf{B}\mathbf{a} \tag{21}$$

and using the constitutive equation equation (12), and equation (21), the final system of equations for the coupled problem can now be written as

$$\begin{aligned} \mathbf{M}\frac{\mathrm{d}}{\mathrm{d}t}\mathbf{a} + (\mathbf{K} + \bar{\mathbf{K}} + \bar{\bar{\mathbf{K}}})\mathbf{a} + \mathbf{f} &= 0 \\ \bar{\mathbf{M}}\frac{\mathrm{d}}{\mathrm{d}t}\mathbf{T} + \mathbf{H}\mathbf{T} + \tilde{\mathbf{f}} &= 0 \end{aligned} \tag{22}$$

where

$$\mathbf{K}_{ij} = \int_\Omega \hat{\mathbf{B}}_i^{\mathrm{T}} \mathbf{D} \mathbf{B}_j \, \mathrm{d}\Omega \tag{23}$$

$$\bar{\mathbf{K}}_{ij} = \int_\Omega (\mathbf{m}^{\mathrm{T}} \hat{\mathbf{B}}_i)^{\mathrm{T}} \lambda \, \mathbf{m}^{\mathrm{T}} \mathbf{B}_j \, \mathrm{d}\Omega \tag{24}$$

$$\mathbf{M}_{ij} = \int \mathbf{W}_i^{\mathrm{T}} \rho \mathbf{N}_j \, \mathrm{d}\Omega \tag{25}$$

$$\bar{M}_{ij} = \int \bar{W}_i \rho c \bar{N}_j \tag{26}$$

$$\mathbf{f}_i = \int_\Omega \mathbf{W}_i^{\mathrm{T}} \mathbf{b}_0 \, \mathrm{d}\Omega - \int_{\Gamma_t} \mathbf{W}_i \bar{\mathbf{t}} \, \mathrm{d}\Gamma \tag{27}$$

$$\bar{f}_i = -\int_\Omega \bar{W}_i Q \, \mathrm{d}\Omega + \int_{\Gamma_q} \bar{W}_i (\bar{q} - \alpha \bar{T}) \, \mathrm{d}\Gamma \tag{28}$$

$$H_{ij} = \int_\Omega \bar{W}_i \rho c \nabla \bar{N}_j (\mathbf{N}\mathbf{a}) \, \mathrm{d}\Omega + \int_\Omega k \nabla \bar{W}_i^{\mathrm{T}} \nabla \bar{N}_j \, \mathrm{d}\Omega + \int_{\Gamma_q} \alpha \bar{W}_i \bar{N}_j \, \mathrm{d}\Gamma \tag{29}$$

$$\bar{\bar{\mathbf{K}}}_{ij} = \int_\Omega \rho \mathbf{W}_i^{\mathrm{T}} (\nabla (\mathbf{N}\mathbf{a})^{\mathrm{T}})^{\mathrm{T}} \mathbf{N}_j \, \mathrm{d}\Omega \tag{30}$$

Equation system (22) can be written as

$$\begin{bmatrix} \mathbf{M} & 0 \\ 0 & \bar{\mathbf{M}} \end{bmatrix} \frac{\mathrm{d}}{\mathrm{d}t} \begin{Bmatrix} \mathbf{a} \\ \mathbf{T} \end{Bmatrix} + \begin{bmatrix} \mathbf{K} + \bar{\mathbf{K}} + \bar{\bar{\mathbf{K}}} & 0 \\ 0 & \mathbf{H} \end{bmatrix} \begin{Bmatrix} \mathbf{a} \\ \mathbf{T} \end{Bmatrix} + \begin{Bmatrix} \mathbf{f} \\ \bar{\mathbf{f}} \end{Bmatrix} = 0 \tag{31}$$

which can be used to solve transient thermally coupled viscoplastic/plastic flow problems. System of equations (31) is highly nonlinear and coupled due to the dependence of matrices $\mathbf{K}$, $\bar{\mathbf{K}}$, $\bar{\bar{\mathbf{K}}}$, $\mathbf{H}$ and $\bar{\mathbf{f}}$ on the velocity and temperature fields.

In general the standard practice of taking

$$\bar{\mathbf{W}} = \bar{\mathbf{N}}; \qquad \mathbf{W} = \mathbf{N} \tag{32}$$

can be used, providing the convective velocities are small. However, this can lead to instability and we have used throughout the optimally 'upwinded' weighting functions[22,23] to obtain best results. This adds little to the computational cost.

It is also worth mentioning here that the convective acceleration terms $\bar{\bar{\mathbf{K}}}$ are in general insignificant in metal forming problems. We have, however, retained these in the solution as the same program is then valid for a wider set of problems. In the solution to be described, very little additional computational time was added due to retaining of convective terms.

STEADY-STATE COUPLED VISCOPLASTIC THERMAL FLOW

In the problems to be discussed here in detail we have assumed that steady-state conditions prevail, i.e. that

$$\frac{\mathrm{d}}{\mathrm{d}t} \mathbf{a} = 0; \qquad \frac{\mathrm{d}}{\mathrm{d}t} \mathbf{T} = 0 \tag{33}$$

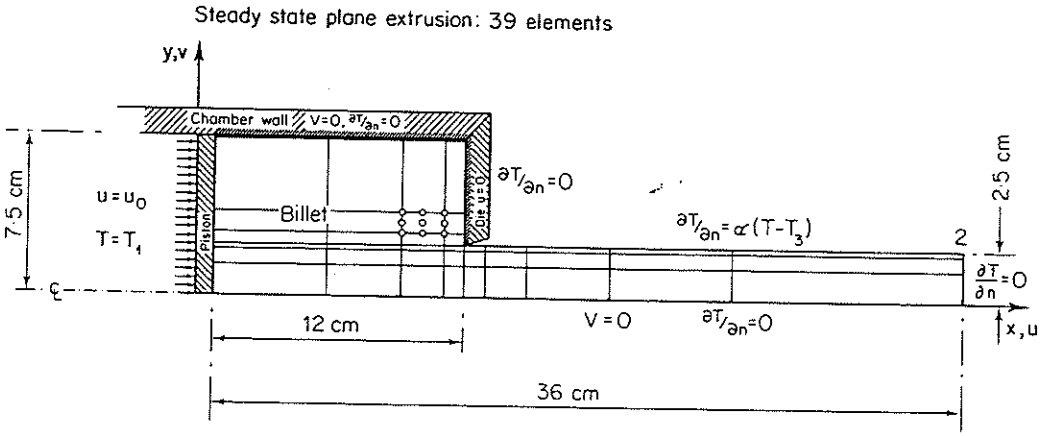

Figure 1. Plane extrusion: full slip boundary

Now the system of equations (21) reduces to

$$\begin{bmatrix} \mathbf{K}, +\bar{\mathbf{K}}, +\bar{\bar{\mathbf{K}}}) & 0 \\ 0 & \mathbf{H} \end{bmatrix} \begin{Bmatrix} \mathbf{a} \\ \mathbf{T} \end{Bmatrix} + \begin{Bmatrix} \mathbf{f} \\ \bar{\mathbf{f}} \end{Bmatrix} = 0 \tag{34}$$

or $\mathbf{Ab}+\mathbf{c}=0$.

The solution process can now be attempted iteratively. In the examples shown in this paper we have used a direct iteration scheme giving for the nth iteration

$$\mathbf{b}_n \equiv \begin{Bmatrix} \mathbf{a} \\ \mathbf{T} \end{Bmatrix}_n = -\mathbf{A}_{n-1}^{-1}\mathbf{f}_{n-1} \tag{35}$$

The temperature dependence of the material properties is taken into account together with the velocity dependence after each iteration defines a new set of material properties applicable in the next iteration. The iteration process stops when some error norm is satisfied. It is

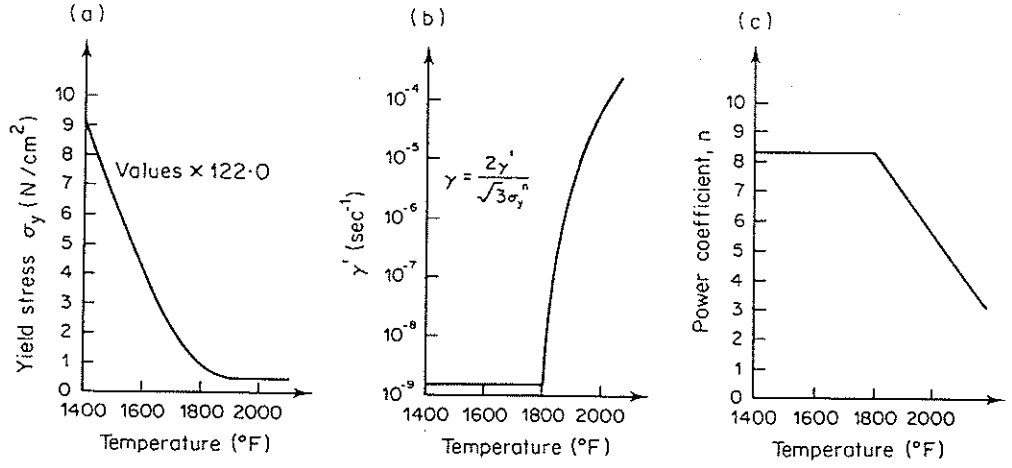

Figure 2. The yield stress, σ_y; the fluidity parameter γ, and the power coefficient n as a function of temperature

important to estimate the error norm separately for velocities and temperature due to their widely different values. In this paper the convergence of iterations is judged using an Euclidean norm with an appropriate factor, i.e. requiring that iteration stops when

$$\begin{aligned} \sqrt{(\mathbf{a}_{n+1}-\mathbf{a}_n)^{\mathrm{T}}(\mathbf{a}_{n+1}-\mathbf{a}_n)} &\leqslant \varepsilon\sqrt{(\mathbf{a}_n^{\mathrm{T}}\mathbf{a}_n)} \\ \sqrt{[(\mathbf{T}_{n+1}-T_n)^{\mathrm{T}}(\mathbf{T}_{n+1}-T_n)]} &\leqslant \varepsilon\sqrt{(\mathbf{T}_n^{\mathrm{T}}\mathbf{T}_n)} \end{aligned} \tag{36}$$

Here $\varepsilon = 0{\cdot}01$ has been taken.

Some points in the solution procedure need to be mentioned here:

1. Matrices $\mathbf{K}$ and $\bar{\mathbf{K}}$ are non-symmetric due to the presence of convective terms, whereas matrices $\mathbf{K}$ and $\bar{\mathbf{K}}$ are symmetric if $\mathbf{W} = \mathbf{N}$ (see equations (23)–(25) and (27), and in this paper

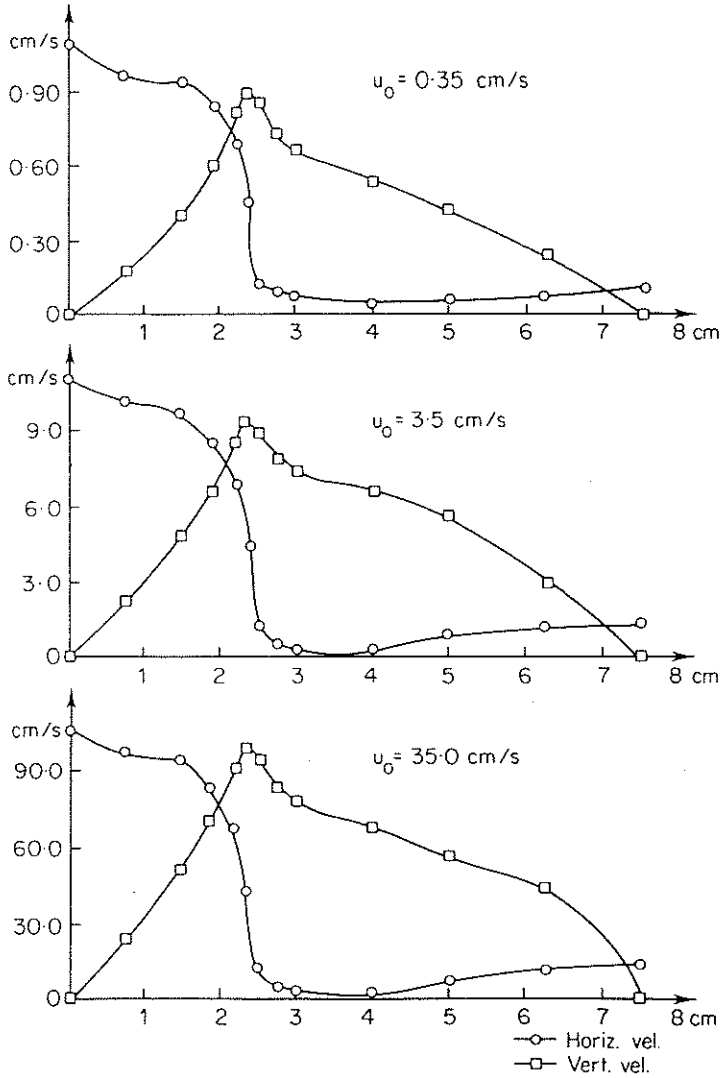

Figure 3. Velocity profiles along A—A ($x = 11{\cdot}5$ cm)

a non-symmetric equations solver has been used in the simultaneous solution of system of equations (34). However, for creeping flow situations, separate solutions for each of the equations represented in equation (34) are possible, thus taking advantage of the symmetry of the matrices $\mathbf{K}$ and $\bar{\mathbf{K}}$. The simultaneous solution, however, has the advantage that both convective and creeping solutions can be incorporated in a single program without adding any extra cost to the solution.

2. If the dependence of the material properties on temperature is very pronounced, oscillations and lack of convergence can occur. This may require some under-relaxation procedure and in our computations in such cases we have used one-half of the temperature change to estimate the viscosities for next iteration, thus reducing the oscillations.

3. Finally, we note that for the examples shown in this paper a nine-noded biquadratic isoparametric Lagrangian element[7] has been used for velocity interpolation with a selective integration scheme (3×3 Gauss quadrature except for the penalty term matrix, $\bar{\mathbf{K}}$, in which 2×2 quadrature is used to relax the constraint imposed by the incompressibility in the overall 'stiffness' matrix.[11,20] For temperature interpolation the same kind of elements have been used and a full 3×3 Gauss quadrature has been employed for all terms of $\mathbf{H}$ since no penalty term is involved.

EXAMPLES

Plane extrusion of Ti–6Al–4V

The first example is a steady-state plane extrusion problem at high temperature with material properties very sensitive to temperature. The geometry, finite element mesh and boundary conditions are shown in Figure 1. Frictionless walls have been assumed and steady-state free

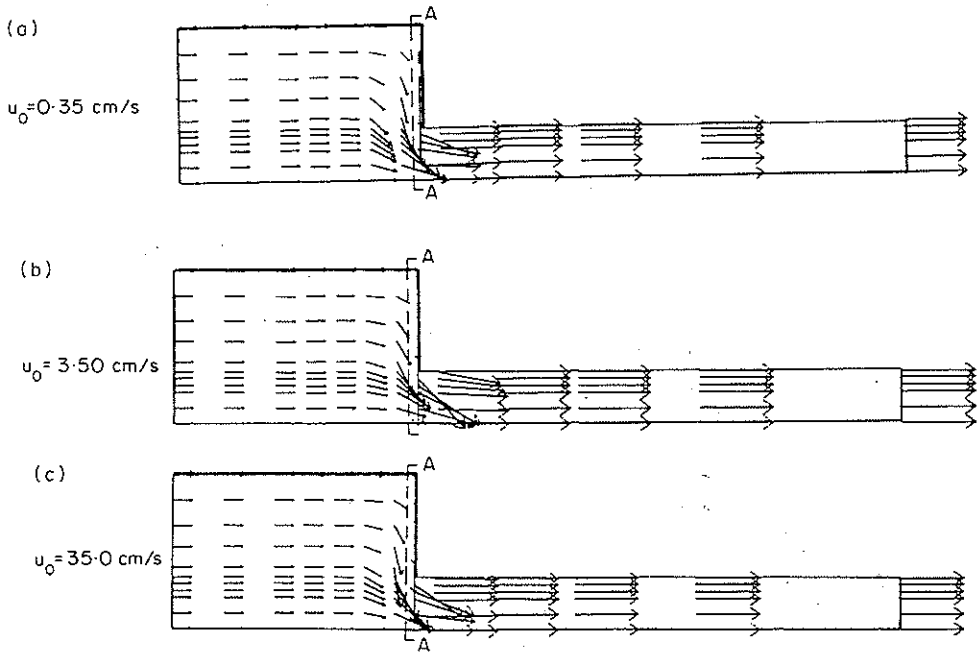

Figure 4. Computed velocity fields for various entry velocities

surface conditions have been treated adjusting the surface co-ordinates as suggested by Zienkiewicz *et al.*[16] The temperature at the upstream boundary, T_1, is prescribed to 1750°F, whereas at the downstream boundary a boundary condition of zero temperature gradient, $\partial T/\partial n = 0$, is imposed. The free surface has been considered here as insulated (i.e. $\alpha = 0$). The problem has been studied for three different ram velocities of 0·35, 3·5 and 35·0 cm/sec. The physical properties of the material can be found in Appendix I. Also, in Figure 2 the temperature dependence of some material properties has been plotted.

Results for the computed velocity fields and for the temperature profiles along $y = 2{\cdot}5$ cm for the three different entry velocities can be seen in Figures 3, 4(a)–(c) and 5, respectively. We note that an increase in the velocity at entry causes an increase in the temperature at exit. Also, in Figure 5 results for the temperature profiles for a constant viscosity corresponding to values of σ_y etc. at $T = 1750$°F are given. These results correspond to the uncoupled solution. The big difference with those obtained using the adequate dependence of the physical properties on temperature shows that the effect of the temperature on the material properties cannot be neglected in the numerical solution without leading to gross errors in the temperature distribution.

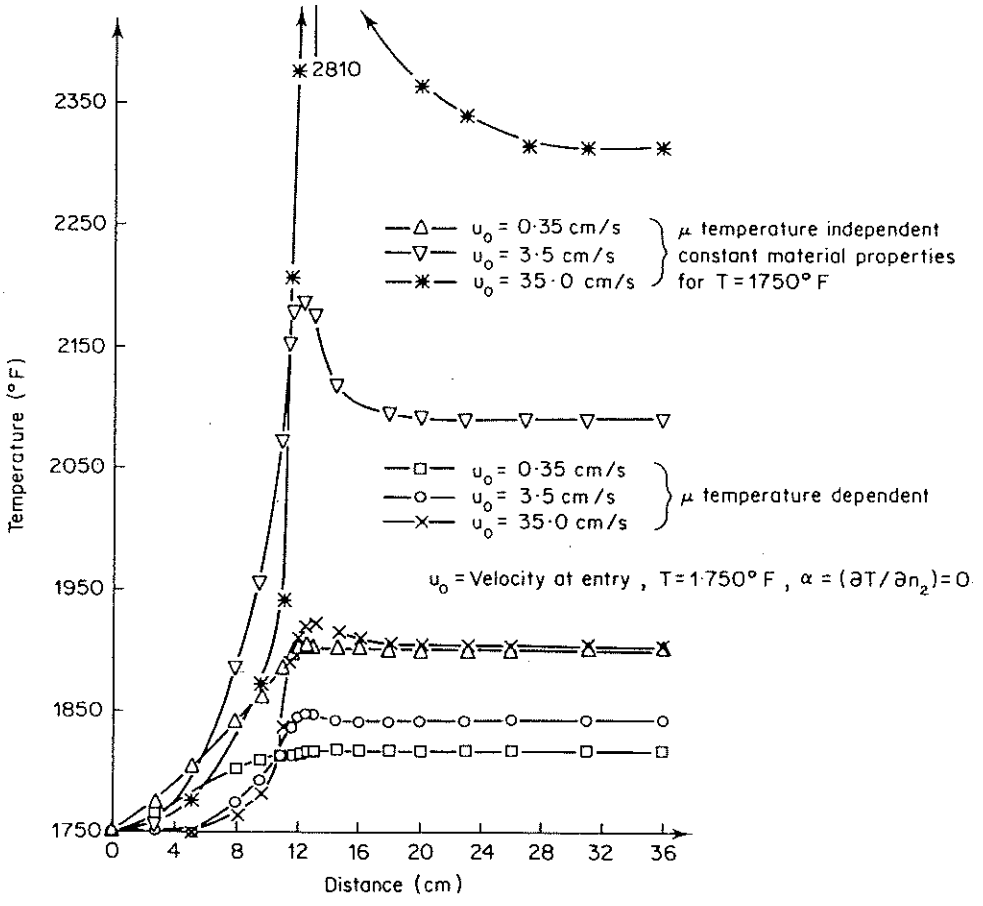

Figure 5. Temperature profiles along $y = 2{\cdot}5$ cm for different entry velocities

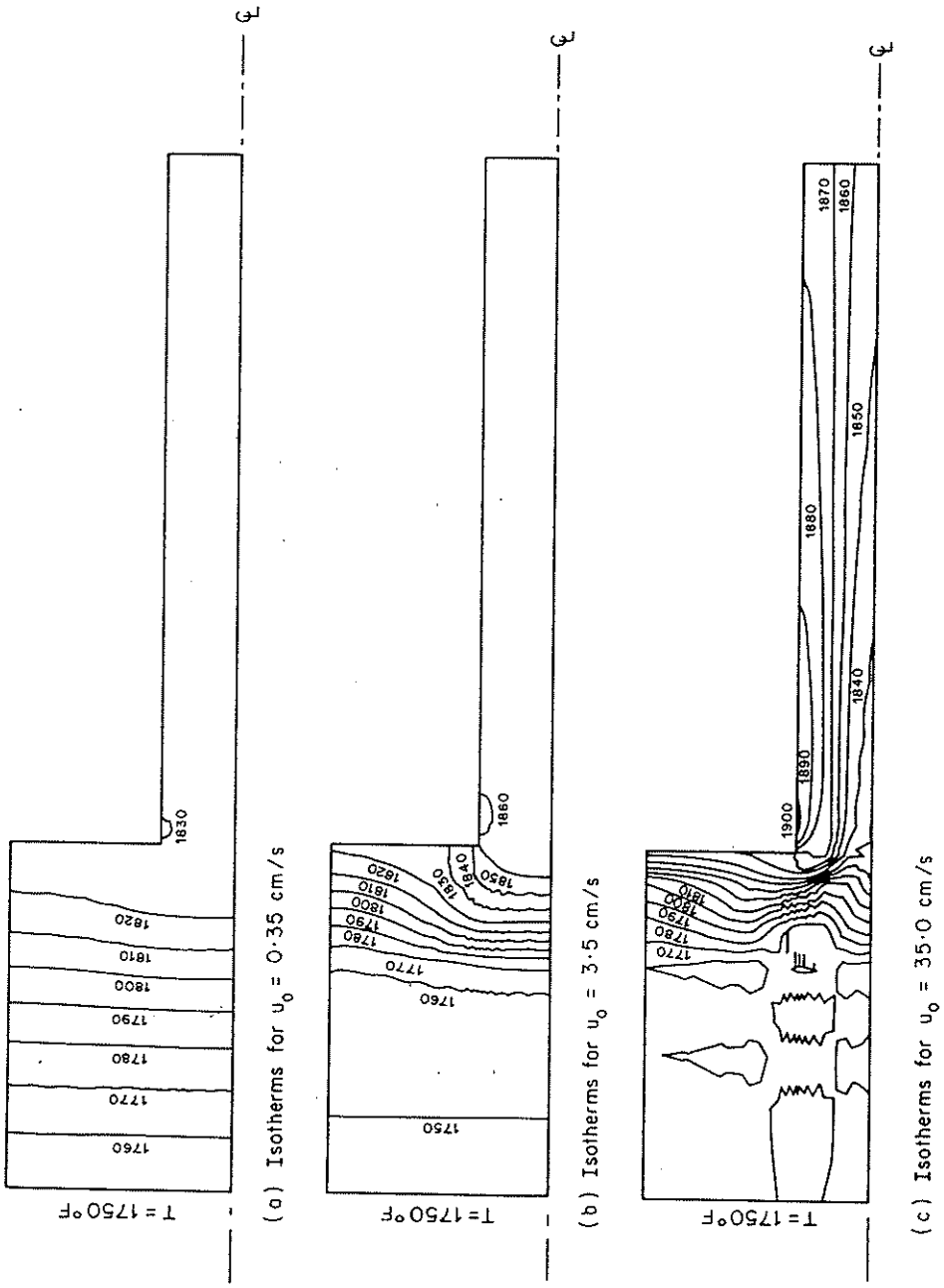

Figure 6. Isotherms for various entry velocities

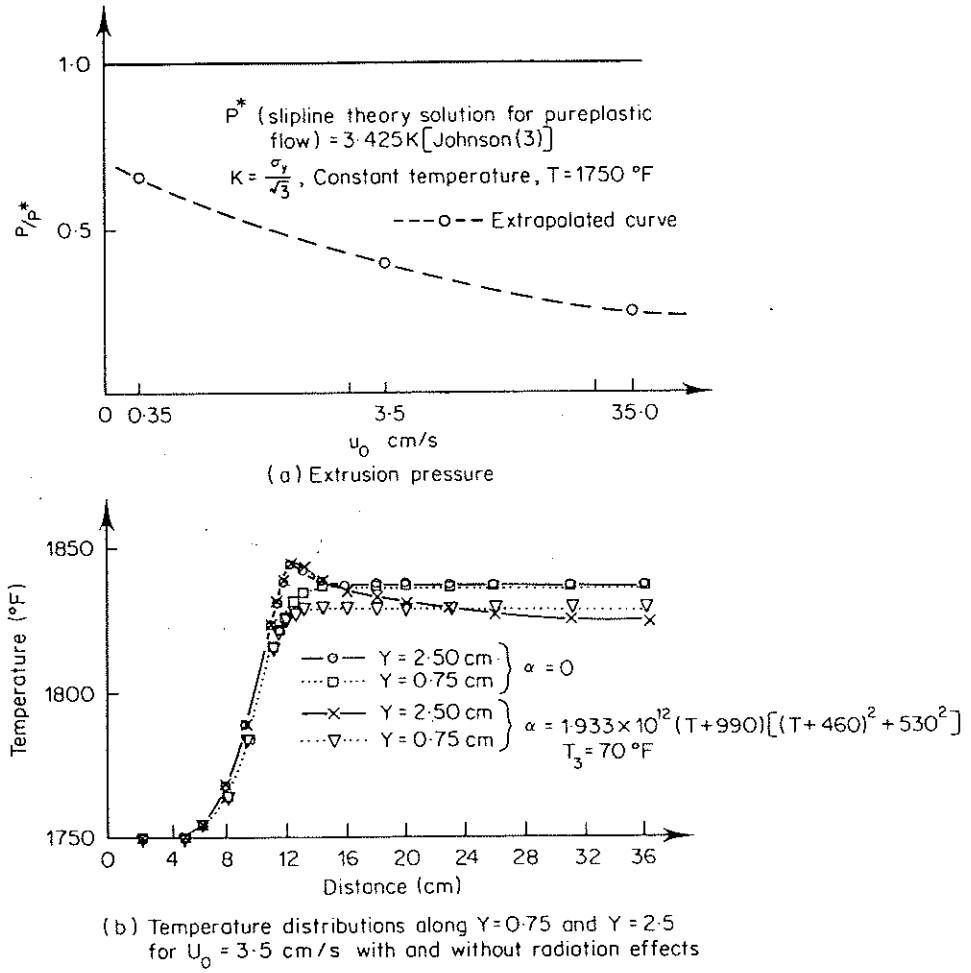

Figure 7. Extrusion pressure and effect of radiation

Figures 6(a)–(c) show the isotherms for each of three entry velocities and again the three different temperature patterns show the big effect of the ram velocity on the temperature distribution.

The extrusion pressure depends also on the velocity at entry for the coupled problem. Figure 7(a) shows the values of the extrusion pressure for the three different ram velocities. Also in the same figure the extrusion pressure obtained with the slip line solution for pure plastic flow with constant yield for $T = 1750°F$ is shown for comparison.

The effect of taking into account radiation effects has also been studied. The value of the radiation coefficient, α, has been taken as a function of temperature and given by the expression shown in Figure 7(b). This dependence of α on temperature adds no extra difficulties to the problem and simply required its value to be updated at the end of each iteration according to the temperature values obtained. The ambient temperature, $\bar{T}$, has been taken equal to 70°F. The effect of radiation can be seen in Figure 7(b) and as expected causes the temperature near the surface to drop.

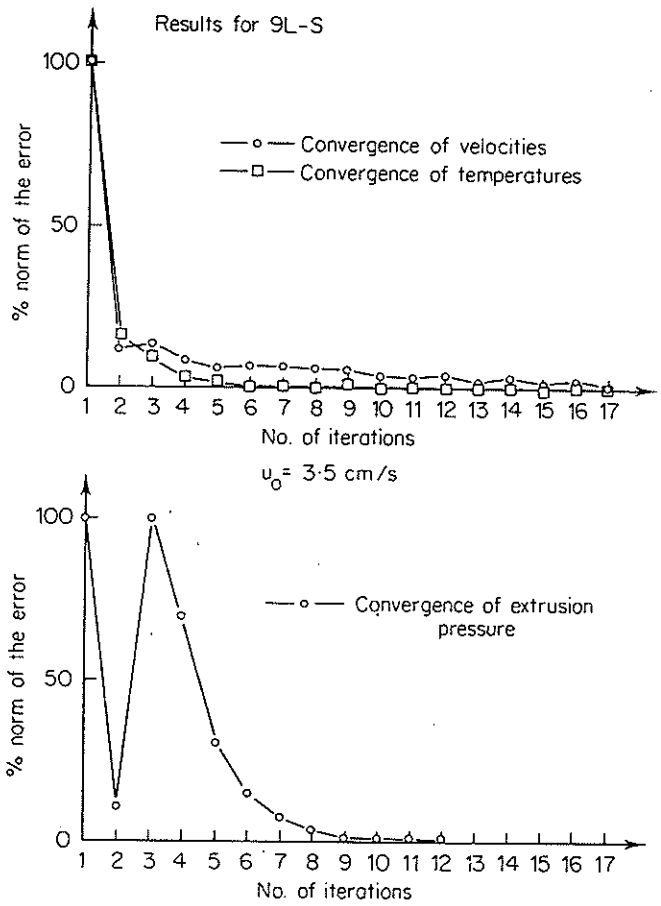

Figure 8. Convergence of velocities, temperature and extrusion pressure for coupled temperature/flow plane strain extrusion problem

Finally, the convergence of the velocity field and that of the extrusion pressure for a ram velocity of 3·5 cm/sec can be seen in Figure 8. It is worth noting that due to the high dependence of the yield stress of the temperature, it has been necessary to make use of the under-relaxation mentioned at the end of last section. The temperature field converges more rapidly than the velocity field and only five iterations were needed to achieve convergence, whereas 13 iterations were needed for the convergence of the velocities. It is worth noting that the convergence of the solution with and without convective terms is exactly the same for this problem.

Hot rolling of a rectangular slab

The process of rolling is, obviously, one of fundamental importance in metal forming. Clearly, in general the problem is not one of steady-state flow, but if the sheet rolled is of long extent it can be approximated as such.

The example chosen here is a plane strain hot rolling problem with the yield stress dependent on temperature. The problem domain, boundary conditions, finite element discretization and

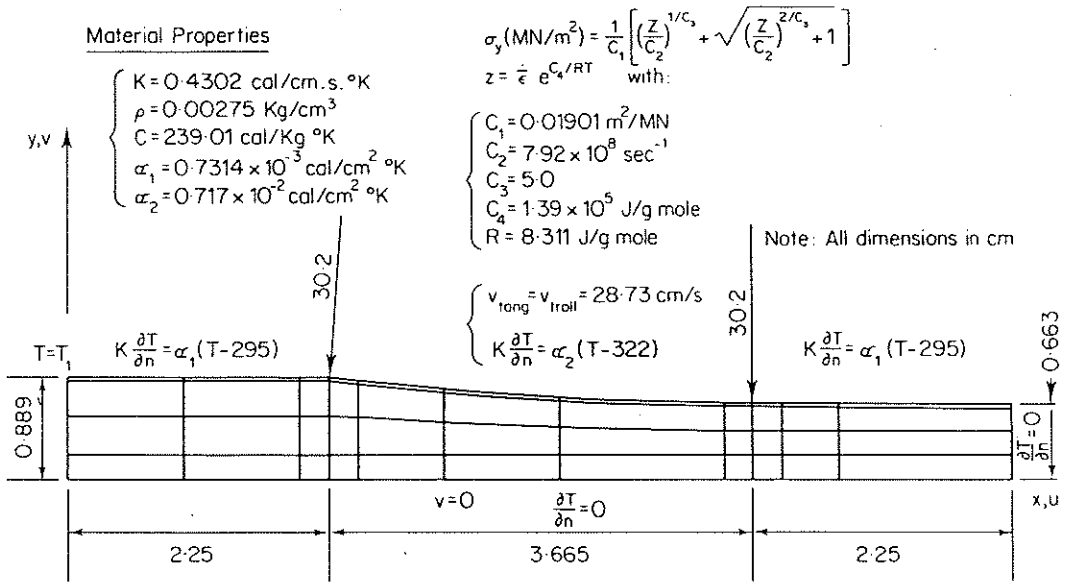

Figure 9. Geometrical configuration boundary conditions and finite element mesh used in hot rolling problem

material properties are shown in Figure 9. Two separate solutions, one using the creeping flow formulation and the other taking into account the acceleration terms, have been carried out.

The numerical computation does not take into account roll deformation, but friction effects between roll and slab surfaces have been considered, following the procedure suggested by Zienkiewicz *et al.*,[16] by imposing a direct proportionality between the pressure, p, and the yield strength, σ_y, in a boundary zone defined by narrow elements. In these

$$\sigma_y = \begin{cases} |\eta p| & \text{if } |\eta p| < \bar{\sigma}_y \\ \bar{\sigma}_y & |\eta p| \geq \bar{\sigma}_y \end{cases}$$

where η is the friction coefficient and $\bar{\sigma}_y$ is the uniaxial yield stress. In this example, friction conditions have been imposed using the above equation for the yield stress values for the thin layer of elements in contact with the roll surface (see Figure 9).

The problem has been studied for two different entry temperatures of 700 and 400 K, respectively. Results obtained with and without convective terms for both velocities and

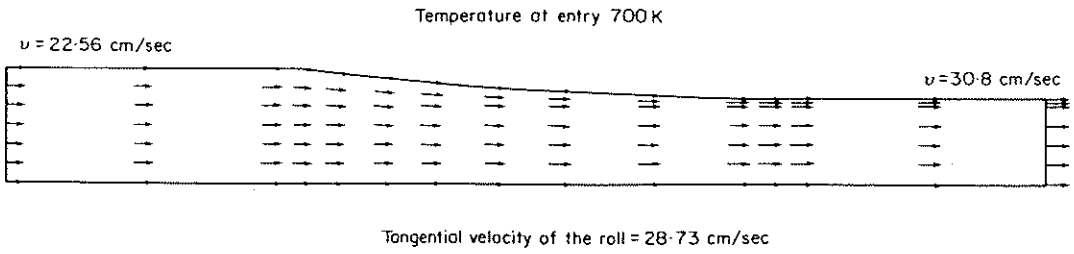

Figure 10. Computed velocity field—rigid contact between roll and slab assumed

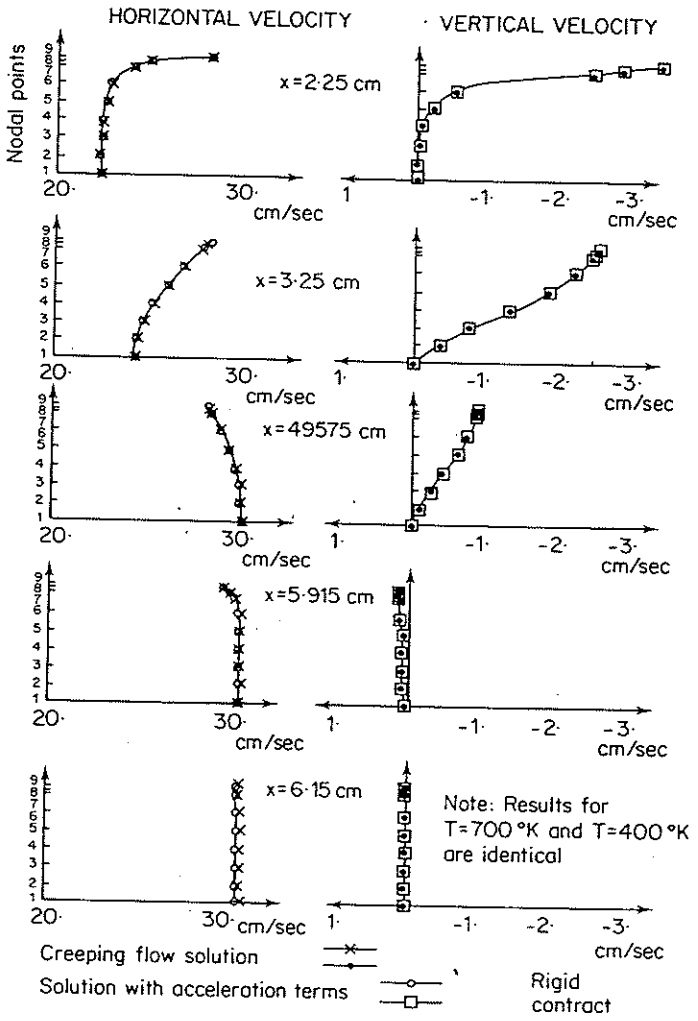

Figure 11. Horizontal and vertical velocity profiles

temperature are nearly identical. The computed velocity field for both temperatures agree within 0·1 per cent and it is shown in Figure 10. The horizontal and vertical velocities across several sections for the rigid contact case have been plotted in Figure 11.

Figures 12(a) and 12(b) show the temperature contours for both entry temperatures, respectively.

The temperature profiles along the slab surface are shown in Figure 13.

The roll force has been assumed to act midway along the angular arc of contact and be directed towards the roll centre. With these assumptions, the roll force per unit width is made up of the resolved components of the nodal forces in contact with the roll in that direction. The roll torque has been obtained considering the moments of such forces about the roll centre.

Figure 14 shows the values of the roll force and roll torque for different friction coefficients between slab and roll.

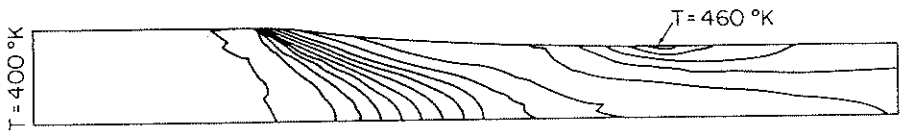

Figure 12(a). Temperature contours for entry $T = 400$ K at intervals $\Delta T = 4{\cdot}0$ K.

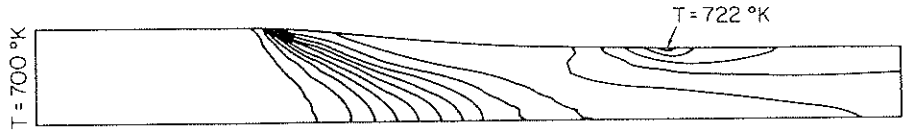

Figure 12(b). Temperature contours for entry $T = 700$ K at intervals $\Delta T = 1{\cdot}5$ K

Convergence of the process is faster than in the previous example due to the dependence of the yield stress on temperature being less pronounced here. Four and three iterations were needed for the convergence of the velocity and temperature fields, respectively, whereas nine iterations were needed for the convergence of the roll force and roll torque values.

CONCLUDING REMARKS

The methods presented in this paper show how a series of previously unsolved problems involved in metal forming can be effectively solved. Obviously extensions to differing configurations and to three-dimensional treatment can be made without difficulties. Much detailed

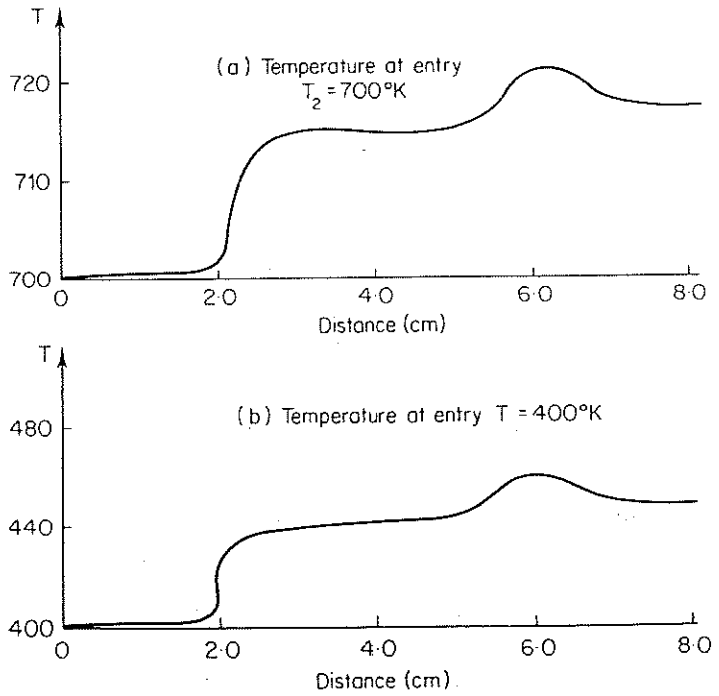

Figure 13. Temperature profiles

	0·01	0·1	0·5	Rigid contact	T_1 °K
Roll Force kN	52·51 22·41	100·73 34·54	129·73 45·85	138·33 52·14	400 700
Roll Torque kN×cm/cm	66·71 34·45	202·77 70·53	262·31 92·75	283·60 104·89	400 700

Figure 14. Roll force and roll torque for various friction coefficients

research work is now required to study practical problems with differing thermal properties and to deal with more complex configurations. As we have said at the outset, elastic effects have been here excluded—but as shown by Shimazeki and Thompson[24] such effects can be incorporated in the basic flow formulation if required.

ACKNOWLEDGEMENTS

The authors would like to thank the Alcoa Foundation of the U.S.A. for the financial support of E. Oñate.

APPENDIX I

Material properties of Ti–6Al–4V (Reference 15)

Temperature-independent properties:

$$\rho = 4598{\cdot}0 \text{ kg/cm}^3$$

$$c = 83{\cdot}4 \text{ cal/kg°F}$$

$$k = 1{\cdot}54 \text{ cal/cm.s.°F}$$

$$J = 418{\cdot}4 \text{ N} \times \text{cm/cal.}$$

Temperature-dependent properties:

$$\gamma = \frac{2\gamma'}{\sqrt{(3)}\sigma_y^n} \qquad \text{(see equation (6))}$$

where

$$\sigma_y \text{ (N/cm}^2) \begin{cases} = 794{\cdot}0 + 0{\cdot}0036 \times (T-1500)^2 - 3{\cdot}25 \times (T-1500); \\ = 1400 \leqslant T \leqslant 1950°\text{F} \\ = 61{\cdot}0; \qquad T \leqslant 1950°\text{F} \end{cases}$$

$$n \begin{cases} = 8{\cdot}2497; \qquad T \leqslant 1800°\text{F} \\ = 8{\cdot}2497 - 1{\cdot}37596 \times 10^{-2} \times (T-1800); \; 1800 \leqslant T \leqslant 2100°\text{F} \\ = 4{\cdot}1218; \qquad T \leqslant 2100°\text{F} \end{cases}$$

$$\gamma' \begin{cases} = 0{\cdot}343485 \times 10^{-8}; \qquad T \leqslant 1800°\text{F} \\ = 0{\cdot}343485 \times 10^{-8} + 0{\cdot}342532 \times 10^{-15} \times (T-1500)^5; \; 1800 \leqslant T \leqslant 2100°\text{F} \\ = 0{\cdot}832265 \times 10^{-3} + 0{\cdot}294604 \times 10^{-10} \times (T-1500)^5; \; 2100 \leqslant T \leqslant 2240°\text{F} \\ = 1{\cdot}58535; \qquad T \leqslant 2240°\text{F} \end{cases}$$

REFERENCES

1. G. Y. Goon, P. I. Poluchin, W. P. Poluchin and B. A. Prudcowsky, *The Plastic Deformation of Metals*, Metallurgica, Moscow (in Russian), 1968.
2. O. C. Zienkiewicz and P. N. Godbole, 'Flow of plastic and visco-plastic solids with special reference to extrusion and forming processes', *Int. J. num. Meth. Engng* **8**, 3–16 (1974).
3. O. C. Zienkiewicz and P. N. Godbole, 'Viscous incompressible flow', *Int. Conf. on Finite Element Methods in Flow Problems*, Swansea, 1974 (Eds. R. H. Gallagher, J. T. Oden, C. Taylor and O. C. Zienkiewicz), Wiley, 1975.
4. O. C. Zienkiewicz and P. N. Godbole, 'A penalty function approach to problems of plastic flow of metals with large surface deformation', *J. Strain Anal.* **10**(3), 180–185, I. Mech. E. (1975).
5. G. C. Cornfield and R. H. Johnson, 'Theoretical predictions of plastic flow in hot rolling including the effect of various temperature distributions', *J. Iron Steel Inst.* **211**, 567–573 (1973).
6. C. H. Lee and S. Kobayashi, 'New solutions to rigid-plastic deformation problems using a matrix method', *I. Eng. Ind. Trans. A.S.M.E.* **95**, 865 (1973).
7. O. C. Zienkiewicz, 'Viscoplasticity, plasticity, creep and viscoplastic flow (problems of small, large and continuing deformation)', *Int. Conf. on Computational Methods in Nonlinear Mechanics*, Texas, Austin, 1974.
8. R. S. Dunham, 'On application of the finite element method to limit analysis. Computational methods in non-linear mechanics', *Int. Conf. on Computational Methods in NonLinear Mechanics*, Texas, Austin, 1974.
9. J. W. H. Price and J. M. Alexander, 'The finite element analysis of two high temperature metal deformation processes'. *2nd Int. Symp. on Finite Element in Flow Problems*, Santa Margherita Ligure (Italy), pp. 715–728 (June 1976).
10. W. S. Farren and T. I. Taylor, 'The heat developed during plastic extension of metal', *Proc. Roy. Soc. A*, **107**, 422 (1925).
11. E. Oñate, 'Plastic flow in metals', *Ph.D. thesis*, Univ. of Wales, Swansea (1978).
12. J. F. N. Bishop, 'An approximated method for determining the temperature reached in steady-state motion problem of plane strain', *Q. J. Mech. Appl. Math.* **9**, 236 (1956).
13. T. Altan and S. Kobayashi, 'A numerical method for estimating the temperature distributions in extrusion through conical dies', *J. Eng. Ind.* 107–118 (1968).
14. R. E. Medrano and P. P. Gillis, 'Viscoplasticity techniques for determining velocity and strain rate fields during extrusion', *Tech. Rep. No. 21, 70-Met. 10*, College of Engineering, Univ. of Kentucky.
15. A. U. Sulijoadikusomo and O. W. Dillon, Jr., 'Temperature distribution of the axisymmetric extrusion of Ti–6Al–4V', *Internal Rep.*, Univ. of Kentucky, Lexington.
16. O. C. Zienkiewicz, P. C. Jain and E. Oñate, 'Flow of solids during forming and extrusion. Some aspects of numerical solutions', *Int. J. Solids Struct.*, **14**, 15–38 (1978).
17. P. C. Jain, 'Plastic flow in solids (static, quasistatic and dynamic situations including temperature effects)', *Ph.D. thesis*, Univ. College of Swansea (1976).
18. J. C. Heinrich, R. S. Marshall and O. C. Zienkiewicz, 'Penalty function solution of coupled convective and conductive heat transfer', *Proc. Int. Conf.* on *Numerical Methods in Laminar and Turbulent Flow*, Swansea (July 1978).
19. O. C. Zienkiewicz and I. C. Cormeau, 'Viscoplasticity, plasticity and creep in elastic solids—a unified numerical solution approach', *Int. J. num. Meth. Engng*, **8**, 821–845 (1979).
20. O. C. Zienkiewicz, *The Finite Element Method in Engineering Science*, McGraw-Hill, London/New York, 1977.
21. O. C. Zienkiewicz, E. Oñate and J. C. Heinrich, 'Plastic flow in metal forming. (I) Coupled thermal behaviour in extrusion. (II) Thin sheet forming', *Proc. Winter Ann. Mtg* of *A.S.M.E. on Application of Numerical Methods to Forming Processes*, San Francisco (1978).
22. J. C. Heinrich, P. S. Huyakorn, A. R. Mitchell and O. C. Zienkiewicz, 'An upwind finite element scheme for two-dimensional convective transport equations', *Int. J. num. Meth. Engng*, **11**, 131–143 (1977).
23. J. C. Heinrich and O. C. Zienkiewicz, 'Quadratic finite element schemes for two-dimensional convective transport problems', *Int. J. num. Meth. Engng*, **11**, 1831–1844 (1977).
24. Y. Shimazeki and E. G. Thompson, Elasto-viscoplastic flow with special attention to boundary conditions. *Int. J. num. Meth. Engng*, **17**, 97–112 (1981).